

BIOMEDICAL OPTICS

PACS numbers: 42.25.Gy; 87.50.W–; 68.49.-h; 42.62.Be
DOI: 10.1070/QE2013v043n08ABEH015074

Light scattering by a rough surface of human skin. 1. The luminance factor of reflected light

V.V. Barun, A.P. Ivanov

Abstract. **Based on the analytical solution of Maxwell's equations, we have studied the angular structure of the luminance factor of light reflected by the rough skin surface with large-scale relief elements, illuminated by a directed radiation beam incident at an arbitrary angle inside or outside the medium. The parameters of the surface inhomogeneities are typical of human skin. The calculated angular dependences are interpreted from the point of view of the angular distribution function of micro areas. The results obtained can be used for solving direct and inverse problems in biomedical optics, in particular for determining the depth of light penetration into a biological tissue, for studying the light action spectra on tissue chromophores under the in vivo conditions, for developing diagnostic methods of structural and biophysical parameters of a medium, and for optimising the mechanisms of interaction of light with biological tissues under their noninvasive irradiation through skin.**

Keywords: *rough surface, skin, light reflection, reflectance factor, probability density.*

1. Introduction

The study of the radiation fields inside and outside a tissue is the key issue in solving a wide range of biomedical optics problems, such as optimisation of light therapy techniques, laser hyperthermia and optical diagnostics. In the case of noninvasive irradiation of a tissue, light passes through the rough interface between skin and the medium and to some extent changes its angular and energy characteristics. This has an impact on the depth of light penetration, the spatial distribution of the absorbed and scattered radiation power, light action spectra on tissue chromophores, and therefore of interest is to evaluate the influence of the skin surface roughness on the light fields in a biological tissue. The first step in such an evaluation would be to study the properties of radiation reflection and transmission by the surface itself. In addition, the radiation scattered at the medium interface carries information about the parameters of roughness, which enables the development of new approaches to solving the inverse problem – reconstruction of the surface characteristics by optical methods. This is important for cosmetology and dermatology, in particular for assessment of efficacy of various skin care products.

In most papers when the light transfer in a biological tissue is considered theoretically, the tissue surface is assumed smooth. This assumption is due to several factors. First, the solution to the problem of radiation transport in a medium is greatly simplified. Meanwhile, from general physical considerations it is clear that such an assumption may lead to errors in the characteristics of the light fields in a medium. For example, Ivanov and Barun [1] assessed the influence of the surface roughness at the interface between two media on the characteristics of the scattered radiation under different irradiation conditions. The coefficients of reflection and transmission of light by smooth and rough surfaces were shown to differ by 1.5–2 times or more. It is clear that for many optical problems, these differences are very significant. Second, there is clearly a lack of experimental data on the characteristics of the surface roughness of the skin, which could be the basis for a statistical description of its structure. In other words, the corresponding initial physical data are virtually absent at present. This is due to a strong variation of the surface properties caused by the change in the skin type, external conditions, age of the person, physical and physiological condition and many other factors. Third, to study the properties of light scattering (reflection and transmission) by a statistically rough surface of the medium requires special techniques and algorithms.

Light fields in biological tissue with the skin roughness taken into account were studied in [2–5] by the Monte Carlo method. Given were specific statistical characteristics of the surface, which was considered as a Fresnel boundary with the reflection and transmission coefficients, defined by well-known formulas. The properties of the interface were accounted for numerically by imitating refraction and reflection on it in the simulations of the trajectories of the photons. It follows from the general theory of radiation scattering by a statistically rough surface [6, 7] that such a description of the light field is valid for surfaces with large-scale inhomogeneities whose dimensions are much larger than the wavelength (the geometrical optics approximation). The authors of papers [6, 7], based on Maxwell's equations, derived an analytical solution for the luminous intensity of the reflected light. By averaging over an ensemble of roughnesses and calculating asymptotically the integral by the stationary phase method [8], it was shown [6, 7] that electromagnetic waves diffracted by large-scale relief elements over directions other than the specular one experience destructive interference and

V.V. Barun B.I. Stepanov Institute of Physics, National Academy of Sciences of Belarus, prosp. Nezavisimosti 68, 220072 Minsk, Belarus; Belarusian State University of Informatics and Radioelectronics, ul. Brovki 6, 220013 Minsk, Belarus; e-mail: barun@dragon.bas-net.by;
A.P. Ivanov B.I. Stepanov Institute of Physics, National Academy of Sciences of Belarus, prosp. Nezavisimosti 68, 220072 Minsk, Belarus; e-mail: ivanovap@dragon.bas-net.by

Received 30 November 2012
Kvantovaya Elektronika **43** (8) 768–776 (2013)
Translated by I.A. Ulitkin

quench each other. The scattered light field is different from zero only in the specular reflection directions, determined by the local angle of incidence of radiation on the surface roughness. Only after such a rigorous justification based on the most common physical principles, Fresnel's formulas can be applied (see, e.g. [2–5]).

Among the publications on the scattering of electromagnetic waves by randomly inhomogeneous surfaces of biological tissues, of interest is paper [9]. On the basis of Maxwell's equations with the Leontovich boundary conditions [10], Rogatkin [9] obtained an analytical solution to the problem of the angular intensity distribution of light reflected from the rough skin surface. However, the conditions [10] are generally applicable only to metal surfaces and for biological tissues they permit estimating the angular structure rather than the absolute values of the reflected light intensity at normal incidence radiation on a macro surface [9, 11]. Furthermore, formulas in [9] follow directly from the general solution [6, 7] for large-scale roughness without additional assumptions.

The aim of this paper is to study the polar and azimuthal structure of the luminance factor (i.e., the characteristics of the light field in absolute units) of a randomly inhomogeneous surface of the skin irradiated by a beam at an arbitrary angle.

2. Statistical characteristics of the skin surface

It is generally assumed in theoretical work that the surface height profiles can be specified by using a random stationary differentiable function $z = \zeta(x, y)$ with a mean value $\langle\zeta\rangle = 0$ with respect to the macro surface plane $z = 0$. We assume that the surface characteristics are not dependent on the azimuth, so that $z = \zeta(r)$, where $r = |\boldsymbol{r}|$, $\boldsymbol{r} = \{x, y\}$. When considering the passage of light through the skin surface, $\zeta(r)$ is sometimes expressed by the Gaussian height distribution function [2, 6, 7, 9]

$$w(\zeta) = \frac{1}{\sqrt{2\pi D_\zeta}} \exp\left(-\frac{\zeta^2}{2D_\zeta}\right) \tag{1}$$

and the correlation function of type

$$K(\tau) = D_\zeta \exp\left(-\frac{\tau^2}{T^2}\right), \tag{2}$$

where T is the correlation length. It follows from (1) and (2) that the two-dimensional vector of random surface slopes, $\boldsymbol{\gamma} = \{\gamma_x, \gamma_y\} = \{\tan\alpha_x, \tan\alpha_y\} = \nabla\zeta(\tau)$, is also distributed by the normal law

$$W(\gamma) = \frac{1}{2\pi D_\zeta} \exp\left(-\frac{\gamma^2}{2D_\zeta}\right), \tag{3}$$

where $\gamma = |\boldsymbol{\gamma}| = \mathrm{d}z/\mathrm{d}r$ is the slope of the tangent to the plane $z = 0$; and $D_\gamma = 2D_\zeta/T^2$. Below, the surfaces characterised by functions (1)–(3) are called Gaussian.

In some papers [3–5, 7], the surface profile is given in the form of a quasi-periodic random function

$$z = \zeta(r) = \zeta_\mathrm{m} \sin(\omega\tau + \theta), \tag{4}$$

where ζ_m and ω take on fixed values; and θ is a random phase uniformly distributed on the segment $[0, 2\pi]$. It is easy to show that for this function, the probability densities of heights and slopes, as well as the correlation function have, respectively, the form:

$$w_\mathrm{s}(\zeta) = \begin{cases} \dfrac{1}{\pi\sqrt{\zeta_\mathrm{m}^2 - \zeta^2}} & \text{at } |\zeta| \leqslant \zeta_\mathrm{m}, \\ 0 & \text{at } |\zeta| > \zeta_\mathrm{m}, \end{cases} \tag{5}$$

$$W_\mathrm{s}(\gamma) = \begin{cases} \dfrac{1}{\pi\sqrt{\gamma_\mathrm{m}^2 - \gamma^2}} & \text{at } |\gamma| \leqslant \gamma_\mathrm{m}, \\ 0 & \text{at } |\gamma| > \gamma_\mathrm{m}, \end{cases} \tag{6}$$

$$K_\mathrm{s}(\tau) = 0.5\zeta_\mathrm{m}^2 \cos(\omega\tau), \tag{7}$$

where $\gamma_\mathrm{m} = \omega\zeta_\mathrm{m}$ is the maximum slope of (4) to the plane $z = 0$. For distributions (5) and (6) it is easy to find the variance values for the heights $D_{\zeta\mathrm{s}} = \zeta_\mathrm{m}^2/2$ and slopes $D_{\gamma\mathrm{s}} = \gamma_\mathrm{m}^2/2$ of the sinusoidal profile that can be used for quantitative comparison of the corresponding distributions (1), (3) and (5), (6) by their integral parameters. For example, it is known [7] that when light is reflected from a rough surface with large-scale inhomogeneities, the surface characteristics are included in the expression for the intensity through the probability density of slopes. Then, for the equality $D_\gamma = D_{\gamma\mathrm{s}}$ to hold, it is needed that $\sqrt{D_\zeta}/T = \omega\zeta_\mathrm{m}/2$. In addition, for the relation similar to that for the Gaussian surface to hold between the variances $D_{\zeta\mathrm{s}}$ and $D_{\gamma\mathrm{s}}$, by the correlation length T_s for surface (4) is meant the value $\sqrt{2}/\omega$.

An overview of the statistical characteristics (1)–(7) in theoretical and experimental works is presented in [12]. Below, we will consider only the Gaussian surfaces (1)–(3) with the interval $0 < D_\gamma < 0.45$, covering the interval of changes in the variance D_γ of human skin [12].

3. Calculation formulas

The geometry of the problem is shown in Fig. 1. Let the radiation beam ensuring illuminance E_0 be incident at the angle ψ on a macro surface, located in the plane xy. The azimuth angle φ_0 of the incident beam, measured from the y axis in the direction of the x axis, is set equal to zero. Bass and Fuks [7] showed that for a statistically rough surface with large-scale inhomogeneities, the angular structure of the reflected light intensity without account for the shadowing of the relief elements has the form:

$$I(\chi, \psi, \varphi) = \frac{E_0 S_0}{4\cos\varphi} r_\mathrm{F}(\eta) \frac{q^4}{q_z^4} W\left(\gamma = -\frac{\boldsymbol{q}_\perp}{q_z}\right), \tag{8}$$

where $I(\chi, \psi, \varphi)$ is the luminous intensity of light from the illuminated macro surface of area S_0 as a function of polar (χ) and azimuth (φ) observation angles (Fig. 1); $r_\mathrm{F}(\eta)$ is the Fresnel reflection coefficient depending on the local angle η of incidence of light on micro areas; $q = |\boldsymbol{q}| = |\boldsymbol{\kappa} - \boldsymbol{\kappa}_0|$; $\boldsymbol{\kappa}$ and $\boldsymbol{\kappa}_0$ are the unit vectors along the propagation direction of reflected and incident waves, respectively; and q_z and $\boldsymbol{q}_\perp$ are the projection of the vector $\boldsymbol{q}$ on the z axis and the xy plane. It is easy to make certain that the vector $\boldsymbol{q}$ is always directed along the local normal to the rough surface. Formula (8) is obtained by the tangential plane method [13, 14] that holds [2, 7] at

$$(kR_\mathrm{c})^{1/3} \cos\psi \gg 1, \tag{9}$$

where $k = 2\pi/\lambda$; λ is the wavelength; and R_c is the local radius of curvature of the surface. Condition (9) indicates that the rough surface is sufficiently smooth so that the wave field at each point can be expressed as the sum of the incident field

and the field reflected by the laws of geometrical optics from the plane tangent to the surface at the point of incidence. This approach is very similar to the Kirchhoff method when considering the diffraction of light by an obstacle [7]. Furthermore, in deriving (8) several terms were omitted, which are small under the following conditions [7]:

$$(k\sigma_\zeta q_z)^2 \gg 1 \text{ at } \boldsymbol{q}\bullet\boldsymbol{\gamma}/q_z \leqslant 1, \tag{10}$$

$$(k\sigma_\zeta q_z)^2 \gg (\boldsymbol{q}\bullet\boldsymbol{\gamma}/q_z)^4 \text{ at } \boldsymbol{q}\bullet\boldsymbol{\gamma}/q_z > 1, \tag{11}$$

where $\sigma_\zeta = (D_\zeta)^{0.5}$ is the standard deviation of the height of inhomogeneities and the dot is the scalar product. In the case of a Gaussian surface (1)–(3), the neglected terms can be quite easily [7, 15] introduced into (8), but in order to simplify the calculation formulas, we assume below that conditions (10) and (11) are met.

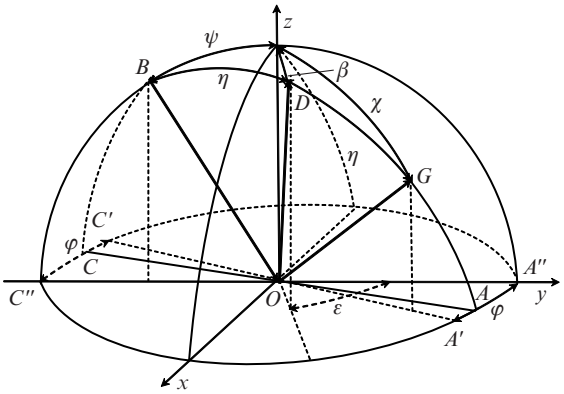

Figure 1. Geometry of the problem.

The argument of the probability density W in (8) shows that the light from the large-scale inhomogeneities is reflected in the specular direction with respect to the plane tangent to the surface at the point of incidence, i.e., according to the laws of geometrical optics. By means of simple geometric constructions it is easy to see that

$$\eta = \arccos\frac{|\boldsymbol{\kappa}\bullet\boldsymbol{\kappa}_0 - 1|}{q}. \tag{12}$$

In illuminating a rough surface, shadow regions are formed that are not involved in the reflection of the incident radiation flux. Moreover, even if a relief element is illuminated, the light reflected from it towards the observer may be blocked by another element. Below we consider the problem of the shadowing effect in the single scattering approximation, i.e., without taking into account multiple reflections between the elements of the surface relief. Bass and Fuks [7] showed that for the electromagnetic-field-quadratic quantities (brightness, luminous intensity and flux) commonly used in optics, the shadowing effect is determined by the parameters $a = \cot\psi/\langle\gamma\rangle$ and $b = \cot\chi/\langle\gamma\rangle$, where $\langle\gamma\rangle = (D_\gamma)^{0.5}$. The asymptotic behaviour of the weak and strong shadowing was analytically described in [7]. In the first of them, $a, b \gg 1$, so that this correction is close to unity, and essentially has no effect on the reflection characteristics. In the opposite case, where $a, b \ll 1$, the shadowing effect is the strongest. The review of the works on the account for rough-surface shadowing is given in [12].

Mathematically, the shadowing effect is described by the correction factor by which it is needed to multiply the reflection characteristics (8) obtained without the shadow regions taken into account:

$$Q(a,b) = [1 + \Lambda(a) + \Lambda(b)]^{-1}, \tag{13}$$

where for the Gaussian surface [16]

$$\Lambda(a) = \frac{1}{2a}\left[\frac{\sqrt{2}}{\pi}\exp(-0.5a^2) - a\operatorname{erfc}\left(\frac{a}{\sqrt{2}}\right)\right]. \tag{14}$$

In the case of weak shadowing ($a, b \gg 1$) we find from (14)

$$\Lambda(a) = \frac{1}{a^3\sqrt{2\pi}}\exp\left(-\frac{a^2}{2}\right) \to 0, \tag{15}$$

so that $Q(a,b) \cong 1$.

We will characterise the angular structure of the reflected light intensity by the luminance factor. This dimensionless characteristic is widely used in photometry [17]. By definition, the luminance factor $\rho(\chi,\varphi,\psi)$ is the ratio of the luminance (intensity) in a given direction (χ,φ) to that of a perfect white Lambertian reflector under the same conditions of illumination. It is easy to show that, given this definition and shadowing effect, the expression for $\rho(\chi,\varphi,\psi)$ is represented by

$$\rho(\chi,\varphi,\psi) = \frac{\pi I(\chi,\varphi,\psi)\,Q(a,b)}{E_0 S_0 \cos\chi}. \tag{16}$$

In the limiting case of a smooth surface, when $D_\gamma \to 0$ and $Q(a,b) \to 1$, based on the approximation of the Dirac delta function [18] we have

$$W(\gamma = -\boldsymbol{q}_\perp/q_z) \to \delta(q_x/q_z)\delta(q_y/q_z) \to$$

$$(q_z)^2\delta(\chi-\psi)\delta(\varphi-\varphi_0)/(\sin\chi\cos\chi),$$

so that we obtain from (16)

$$\rho(\chi,\varphi,\psi) \to \pi r_F(\psi)\delta(\chi-\psi)\delta(\varphi-\varphi_0)/(\sin\chi\cos\chi),$$

i.e., the luminance factor of a smooth Fresnel interface. It is easy to see that the reflection coefficient R of the surface with this luminance factor is $r_F(\psi)$. Indeed, for a smooth surface, using the definition of R [17] under directional illumination, we have

$$R(\psi) = \frac{1}{\pi}\int_0^{2\pi} d\varphi \int_0^{\pi/2} \rho(\chi,\varphi,\psi)\sin\chi\cos\chi d\chi \equiv r_F(\psi).$$

4. The angular distribution function of micro areas

It follows from (8) and (16) that the surface structure defines the final formula for the luminance factor through the probability density of slopes $W(\gamma)$) or $W_s(\gamma)$. The function $W_s(\gamma)$ has a special feature at $\gamma = \gamma_m$. The reasons are discussed in [7]. This feature creates an inconvenience in calculating the characteristics of light reflection from a quasi-periodic surface. Such difficulties can be avoided if we calculate for boundary (4) the luminance factors based on the angular distribution function f of micro areas [17, 19, 20]. Furthermore, the interpretation of the results for the Gaussian surface will

be more physically illustrative in this case. Below, we will use this approach. The relation between the model [17, 19, 20] and the statistical characteristics (1)–(3) is discussed in [12]. By the definition, the specified function is

$$f(\beta,\varepsilon) = \frac{\mathrm{d}\sigma(\beta,\varepsilon)}{S_0 \mathrm{d}\omega}, \quad (17)$$

where S_0 is the macro surface area; $\mathrm{d}\sigma(\beta,\varepsilon)$ is the area of micro areas, the normals to which lie in the solid angle $\mathrm{d}\omega$ around the direction defined by the polar (β) and azimuth (ε) angles (Fig. 1). In the case of the azimuthal symmetry of micro-area distribution, the distribution function depends only on the polar angle β. Let us find the expression for the luminance factor. We consider the light flux reflected from the micro areas $\mathrm{d}\sigma(\beta)$ in the direction OG: $\mathrm{d}F = E_0 \cos\eta \mathrm{d}\sigma(\beta) \times r_\mathrm{F}(\eta)/\cos\psi$. The normal OD to the micro areas is in the reflection plane OBG. The reflected flux is distributed in the solid angle $\mathrm{d}\omega_\mathrm{s}$. Naturally, the angle η of incidence on the micro areas equals the angle of reflection from them. At constant χ and φ, and at the zero angle of incidence, the plane CBA of light reflection from micro areas intersects the macro surface along the line $C'A'$ and at an angle of 90° – along the line $C''A''$. Obviously, the luminance of light reflected from a rough surface in the direction (χ,φ) is

$$B(\chi,\varphi,\psi) = \frac{E_0 \cos\eta \mathrm{d}\sigma(\beta) r_\mathrm{F}(\eta)}{S_0 \cos\chi \cos\psi \mathrm{d}\omega_\mathrm{s}} = \frac{E_0 \cos\eta f(\beta) r_\mathrm{F}(\eta) \mathrm{d}\omega}{\cos\chi \cos\psi \mathrm{d}\omega_\mathrm{s}}, \quad (18)$$

and the luminance of a perfect Lambertian reflector is E_0/π. Hence it follows that

$$\rho(\chi,\varphi,\psi) = \frac{\pi \cos\eta f(\beta) r_\mathrm{F}(\eta) \mathrm{d}\omega}{\cos\chi \cos\psi \mathrm{d}\omega_\mathrm{s}}. \quad (19)$$

It can be shown (see Appendix 1) that, at given angles χ, φ and ψ, the azimuth (ε) and polar (β) angles of the normal to the micro areas are determined from the equations:

$$\tan\varepsilon = \sin\varphi \sin\chi(\cos\psi \cos\chi - \sin\psi \sin\chi \cos\varphi - 1)/A, \quad (20)$$

where

$$A = \sin^2\varphi \sin^2\chi \sin^2\psi + [\sin\chi \cos\psi \cos\varphi + \cos\chi \sin\psi][\cos\chi - \cos\psi], \quad (21)$$

$$\tan\beta = \sin\varphi \sin\psi \sin\chi [\sin\varepsilon \sin\chi \cos\varphi \cos\psi + \sin\varepsilon \sin\psi \cos\chi - \sin\varphi \sin\chi \cos\varepsilon \cos\psi]^{-1}. \quad (22)$$

The angle η of incidence (reflection) of radiation on a micro area is found from (12) or its equivalent expression

$$\cos 2\eta = \cos\psi \cos\chi - \sin\chi \sin\psi \cos\varphi, \quad (23)$$

and the ratio of solid angles (see Appendix 2) is

$$\frac{\mathrm{d}\omega}{\mathrm{d}\omega_\mathrm{s}} = \frac{1}{4\cos\eta}. \quad (24)$$

As can be seen from (24), this ratio is in the range 0.25 to ∞. For example, at large angles ψ of incidence of light on a macro surface and large observation angles χ, when the micro areas, the normals to which are close to the z axis (the angle β is small), are involved in reflection, the angle η is also large. If η varies from 75° to 90°, the ratio of the solid angles ranges from unity to infinity. Large ratios (24) correspond to the cases when at a finite change of the solid angle $\mathrm{d}\omega$ of the micro areas, the angle $\mathrm{d}\omega_\mathrm{s}$ remains almost constant, which is just the case when η is close to 90°. However, one can see from (19) that this feature of ratio (24) does not affect the integrability of the luminance factor. Indeed, substituting (24) into (19), we obtain

$$\rho(\chi,\varphi,\psi) = \frac{\pi f(\beta) r_\mathrm{F}(\eta)}{4\cos\chi \cos\psi}. \quad (25)$$

This formula, similarly to relation (8), with (21)–(23) taken into account, gives the angular structure of light reflected by the rough surface in the direction (χ,φ), based on the concept of the angular distribution function of micro areas. Obviously, in the limiting case of a smooth surface, when $f(\beta) \sim \delta(\beta)$, both formulas (8) and (25) should yield the same result, presented at the end of Section 3. This can be shown using definition (17) and relations (20)–(23). Let us write the relation for $\rho(\chi,\varphi,\psi)$ of a smooth surface in an illustrative manner. It directly follows from the definition of the luminance factor that

$$\rho(\chi \approx \psi, \varphi_0) = \frac{\pi r_\mathrm{F}(\psi)}{\Delta\omega_0 \cos\psi}. \quad (26)$$

Here $\Delta\omega_0$ is the solid angle in which the incident flux is concentrated. Substituting (26) in the definition of the reflection coefficient from the surface with a particular luminance factor, given in Section 3, we obtain $R(\psi) \equiv r_\mathrm{F}(\psi)$, because in this case the solid angle, in which the reflected radiation is trapped, is of the form

$$\Delta\omega_s = \int_0^{2\pi} \mathrm{d}\varphi \int_0^{\pi/2} \sin\chi \mathrm{d}\chi \equiv \Delta\omega_0.$$

From (26), in particular, follows that when $\chi \approx \psi$ and $\varphi \approx 0$, regardless of the degree of surface roughness, the luminance factor is proportional to $r_\mathrm{F}(\psi)/\cos\psi$, since reflection involves only horizontal micro areas that are parallel of the macro surface.

The effect of the shadowing of relief elements can be introduced in (25) similarly to (16). The question of which formula, (8) or (25), should be used in calculations depends on the presence of experimental or other initial data on the probability densities (1), (3) or function (17). Note that the measurement of $f(\beta)$ by a standard optical technique [17, 20] is difficult because the radiation reflected by the skin surface, is overlapped by the light scattered deep in the tissue. Therefore, below we use in the calculations relations (8) and (16), for which there are, although to a limited extent, experimental data [12] obtained by the profilemeter, and formula (25) is convenient for the interpretation of the results.

One more remark concerning relations (8) and (25). By equating their right-hand sides, we can see that the formal relationship of $f(\beta)$ with the characteristic of a rough surface – probability density of slopes $W(\gamma)$ – includes angles of observation and illumination χ, φ and ψ. In other words, probabilistic description of the surface properties (1)–(3) and the angular function distribution $f(\beta)$ of micro areas are two different representations of the statistical properties of the surface. In general, they do not follow from each other. This fact is discussed in detail in [12].

5. Results and discussion

Under external irradiation of the skin its outer surface is illuminated by the radiation source, and the inner surface – by the light scattered deep in the tissue. Therefore, below we consider the luminance factors for the two cases of illumination by a directed beam of light, i.e., when radiation is incident from inside and outside the tissue. The refractive index of the tissue is selected equal to 1.55, which corresponds to the uppermost stratum corneum of the skin in the visible spectral region [21]. First of all, we find out how partial shadowing (shielding) of the surface by the elements of its relief affects the recorded signal. The calculations show that for angles of incidence and reflection of less than 70°, this effect is not observed. However, if one of the angles is greater than 70°, at any other angle this effect to some extent always manifests itself. We also note that in passing to a smoother skin surface, the shielding effect of light on the luminance factor, of course, weakens. All the results below will be presented with the shadowing taken into account, because it does not cause any difficulties.

It was mentioned earlier that the analysis of the results will be more illustrative if use is made of formula (25), which contains three factors depending on the angles $f(\beta)$, $r_F(\eta)$ and $1/(\cos\chi\cos\psi)$. The last of the factors is called trigonometric. Typically, the function $f(\beta)$ is maximal at $\beta = 0$ and decreases with increasing η. For unpolarised light, the reflection coefficient $r_F(\eta)$ continuously increases with increasing η. In the case of the total internal reflection (TIR), it assumes a maximum value equal to unity and does not change with a further growth in η. These obvious features of the angular behaviour of the factors (25) are sufficient for a qualitative explanation of the results given below.

Consider the effect of the skin surface roughness (variance D_γ) on the angular distribution of the reflected light. Figure 2 illustrates this distribution at the azimuth angle $\varphi = 0$ and different angles of incidence inside the skin and outside the tissue depth. For brevity, the luminance factors in the two cases are denoted by $\rho\downarrow$ (dashed curves) and $\rho\uparrow$ (solid curves), respectively. Note here that, for incidence angles 0, 30°, 60° and 80°, the TIR occurs at $\chi \approx 80°$, 50°, 20° and 0.4°, respectively. These TIR angles will, of course, manifest themselves in the

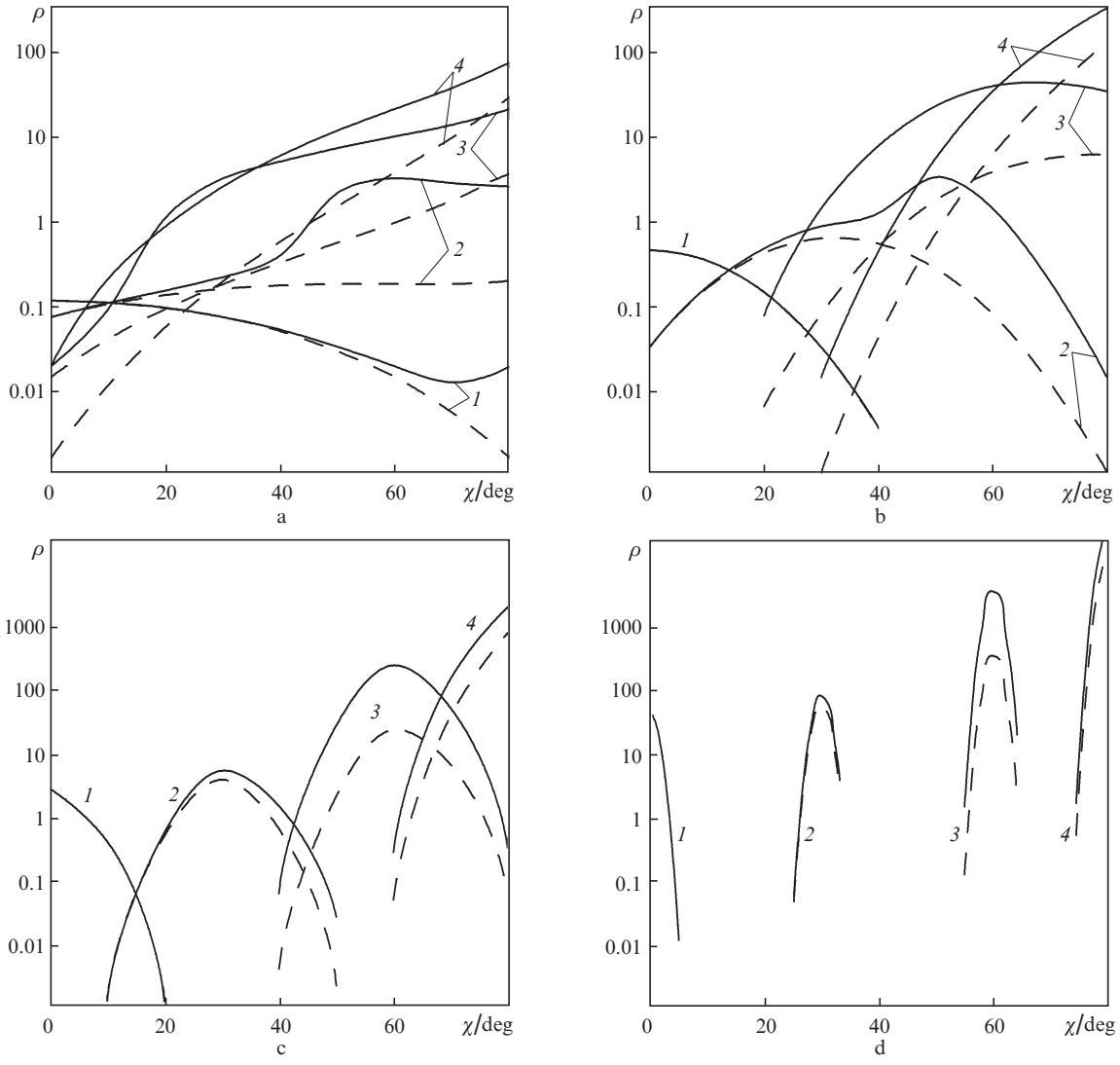

Figure 2. Effects of the roughness degree on the polar structure of the luminance factors of reflected light upon illumination of the medium from outside (dashed curves) and inside (solid curves); D_γ = (a) 0.2, (b) 0.05, (c) 0.013 and (d) 0.0013, ψ = (*1*) 0, (*2*) 30°, (*3*) 60° and (*4*) 80°, $\varphi = 0$.

angular structure of the luminance factor $\rho\uparrow$, as will be discussed below.

We start by analysing the reflection from the surface with $D_\gamma = 0.2$ (Fig. 2a). One can see that in most cases $\rho\uparrow$ is greater than $\rho\downarrow$, which is due to the value of the Fresnel reflection coefficient from the surface micro areas. At $\psi = 0$ and small χ the solid and dashed curves (*1*) coincide, because reflection occurs from nearly horizontal micro areas and their coefficients r_F are the same. With increasing χ, more inclined areas make contribution to the luminance factors, so that the impact of increased r_F and the decrease in the relative number of such areas begin to manifest themselves. The first factor contributes to the increase in the observed signal, and the second – to the reduction. The influence of the second factor is stronger, and as a result ρ decreases. Only at the beginning of the TIR zone ($\chi \approx 80°$) an increase in the signal is observed. One can see from Fig. 2a that with increasing ψ the range of angles of a sharp increase in the luminance factor is shifted to lower values of χ at which TIR takes place. With increasing angle of observation, ρ does not decrease, as in the case to which curve (*1*) corresponds; in this case, we deal with an increase in the luminance factor [curves (*3*) and (*4*)]. This is explained by the fact that on the initial segment χ, the micro areas reflecting light in this direction have the azimuth $\varepsilon = \pi$, i.e., they face the direction of the incident radiation flux. As a result, with increasing χ, the number of such micro areas increases, because their orientation becomes close to horizontal. Furthermore, the Fresnel reflection coefficient grows. With a further increase in χ, when the azimuth ε abruptly changes from π to 0, the three factors in (25) make multidirectional contribution to the luminance factor. Thus, the decrease in the function $f(\beta)$ leads to its reduction, but it is more than compensated by the increase in $r_F(\eta)$ and trigonometric factor. As a result, the luminance factor increases.

The detailed consideration of Fig. 2a and detailed qualitative explanation of the angular dependence of the luminance factors are, naturally, applicable to the cases illustrated in Figs 2b–d. Therefore, we will pay below the main attention to the quantitative relationships and differences of the dependences from those shown in Fig. 2a.

Consider a smoother surface corresponding to $D_\gamma = 0.05$ in Fig. 2b. In this case, at $\psi = 0$, the values of ρ at small observation angles χ are naturally larger than in Fig. 2a. Obviously, this is due to a greater number of the micro areas oriented nearly horizontally. For the same reason, the decrease in the luminance factors [curve (*1*)] with the growth of χ is more noticeable. In the range of the values on the ordinate axis (Fig. 2b) the values of $\rho\uparrow$ and $\rho\downarrow$ are the same, and the TIR takes place outside this range. For $\psi = 30°$ [curves (*2*)] there is a rapid decrease in the luminance factors at $\chi > 50°$. This is due to the strong decrease in the number of inclined micro areas responsible for light reflection. For oblique angles of incidence [curves (*3*) and (*4*)] there is a sharp increase in light when approaching the angle of specular reflection, whereas at small χ the luminance factors are negligible.

When the variance D_γ (Figs 2c and 2d) is further increased, there appear clear maxima of specular reflection corresponding to different angles of incidence of light. It is obvious that the angular width of the maxima depends on the degree of the surface roughness. The smaller the value of D_γ, the narrower the luminance factor maximum. It should be noted that with decreasing D_γ the luminous intensity concentrated in the reflection maxima remains constant, but falls in a smaller range of angles. Therefore, the maximum values of the luminance factor for the smoothest of the surfaces in question ($D_\gamma = 0.0013$) are the highest.

Consider the effect of the angles of incidence and observation at different azimuths on the luminance factor. The relevant data are presented in Fig. 3 for the variance $D_\gamma = 0.44$. At lower values of D_γ similar results are not as illustrative, because in a wide range of the angles φ the luminance factor is very small, but the general laws governing the formation of the reflected light field, of course, remain at any D_γ. Let us first compare the data in Fig. 3a ($\varphi = 0$) and Fig. 3b ($\varphi = 30°$). It is seen that at a fixed angle of incidence ψ, the corresponding curves are similar to each other. This is due to the fact that the degree of the surface roughness is large enough so that the observation azimuth up to 30° weakly affects the angular distribution of the reflected light. With increasing φ the luminance factors transform (Fig. 3c, $\varphi = 90°$). The interpretation of the results is very illustrative at $\varphi = 180°$, shown in Fig. 3d, because here we have simple relationship between the angles that appear in (8) and (25). Indeed, in this case, as seen from Fig. 1, $\eta = 0.5|\psi - \chi|$ and $\beta = 0.5|\psi + \chi|$. One can see from Fig. 3d that at low angles of incidence ψ [curves (*1*) and (*2*)] the luminance factors $\rho\uparrow$ and $\rho\downarrow$ are the same in the region of small observation angles χ, while with increasing ψ [curves (*3*) and (4)] they are the same in the region of large χ. The coincidence of the curves is due to the fact that in both cases, the light is reflected from the micro areas oriented almost horizontally to the incident beam when the Fresnel reflection coefficients for the light incident on the surface from inside and outside the medium are the same. At small angles ψ the angular dependences of $\rho\uparrow$ and $\rho\downarrow$ diverge; the actual values of $\rho\uparrow$ and $\rho\downarrow$ grow in the area of large χ, while at large ψ they grow in the region of small χ. In the first of these cases, the reflection coefficient $r_F(\eta)$ and trigonometric factor increase with increasing χ and the decreasing function $f(\beta)$ does not compensate for this growth. As a result, the luminance factors $\rho\uparrow$ and $\rho\downarrow$ are increased. In the second case, $r_F(\eta)$ and $f(\beta)$ increase with decreasing χ, whereby $\rho\uparrow$ and $\rho\downarrow$ take on large values. Note also that curves (*1*), corresponding to $\chi = 0$, are identical for all azimuths φ, because the angular structure of reflected light is symmetric with respect to the beam incident along the normal to the surface.

To give a complete picture, Fig. 4 shows examples of the azimuthal structure of the luminance factors $\rho\uparrow$ and $\rho\downarrow$ for two polar angles of observation, $\chi = 60°$ and 80°, and some angles of incidence, ψ. Obviously, due to symmetry of the problem at $\chi = 0$ or $\psi = 0$ [curves (*1*) in Figs 4a and b] the values of $\rho\uparrow$ and $\rho\downarrow$ are independent of φ. With the growth of χ the azimuthal structure of the reflected light is dramatically transformed. The larger the values of χ and ψ, the stronger the transformation. There is a general trend – the luminance factors decrease with increasing φ. The qualitative analysis of the azimuthal dependences is possible with the help of (25), but it is similar to that presented above, and therefore we will not give it here.

6. Conclusions

In analysing the angular structure of the luminance factors of light reflected from the rough surface of the skin, we have used the asymptotic solution to Maxwell's equations in the geometrical optics approximation [6, 7]. Its applicability to the optics of the skin is due to the characteristics of its microrelief. A similar analysis based on recalculation of the corresponding angles by Snell's law can be applied to the intensity

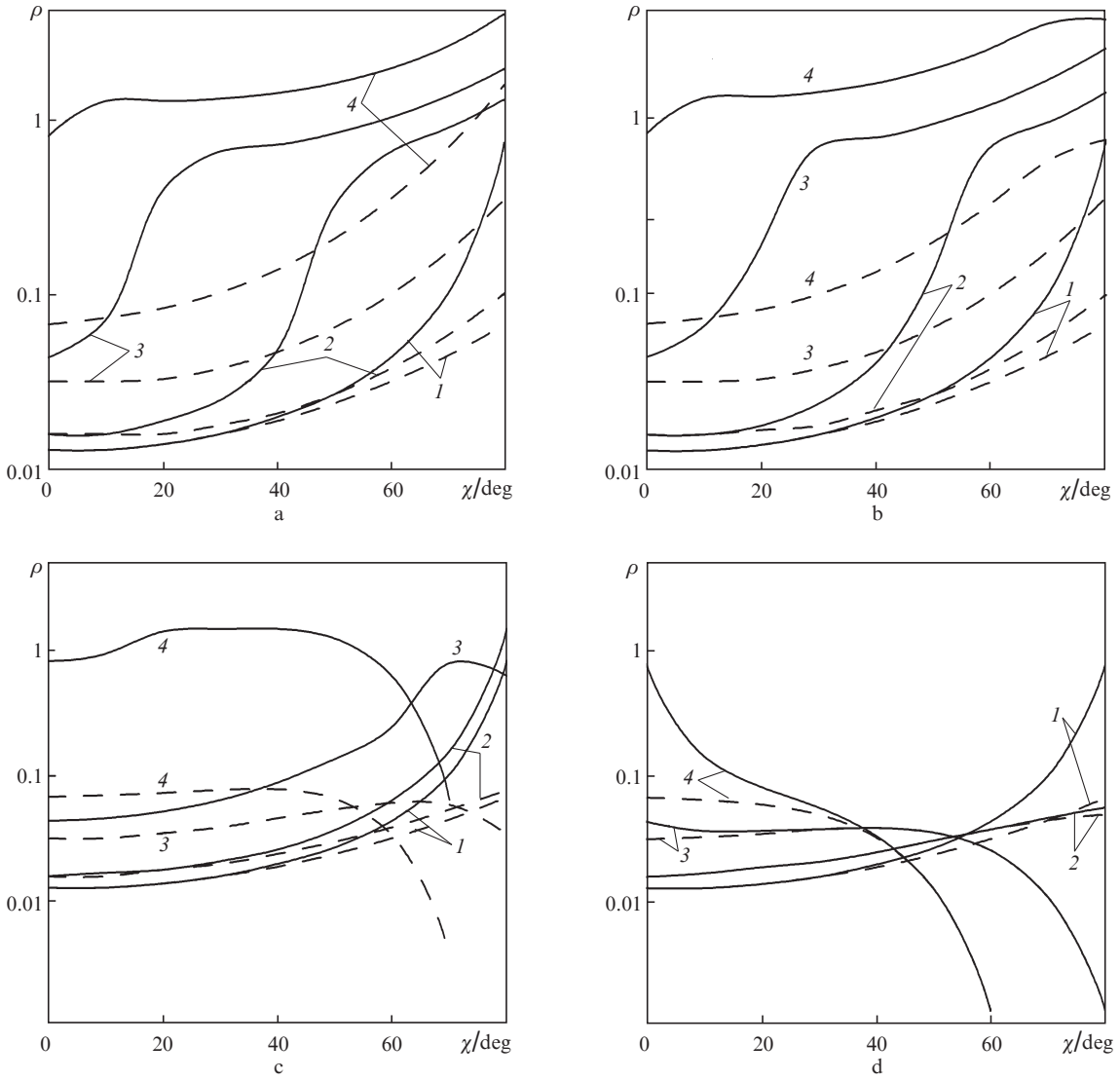

Figure 3. Polar structure of the luminance factors of reflected light upon illumination of the medium from outside (dashed curves) and inside (solid curves); φ = (a) 0, (b) 30°, (c) 90° and (d) 180°, χ = (*1*) 0, (*2*) 30°, (*3*) 60° and (*4*) 80°, $D_\gamma = 0.44$.

of light transmitted by the rough skin surface. We note here that for the radiation beam transmitted through the interface, the argument b of the factor $Q(a,b)$ (13), taking shadowing into account, will contain the angle of refraction instead of the angle χ. The derived formulas can be also used to calculate the luminance factors of the reflected and transmitted polarised radiation under illumination by natural or polarised light. To do this, we should only substitute in the corresponding expressions the required Fresnel coefficient of reflection or transmission of the micro areas. The polarisation state can be arbitrary. The knowledge of the luminance factors in absolute units for the reflected and transmitted light allows one through simple integration to calculate the reflection and transmission coefficients of radiation by the skin surface at an arbitrary angular structure of illumination. These integral characteristics are often used to describe a light field inside and outside the biological tissues, to study the radiation–tissue interaction, to determine the depth of penetration of light in the medium and to solve many other problems of biomedical optics.

Appendix 1

Relationship between the angles β, ε and χ, φ, ψ

As can be seen from Fig. 1, the direction cosines of the vectors $\boldsymbol{\kappa}_0$, $\boldsymbol{\kappa}$ and the unit vector $\boldsymbol{n}$ of the outer normal to the micro area with respect to the axes x, y and z are equal to (0, $\sin\psi$, $-\cos\psi$), ($\sin\varphi\sin\chi$, $\cos\varphi\sin\chi$, $\cos\chi$) and ($\sin\varepsilon\sin\beta$, $\cos\varepsilon\sin\beta$, $\cos\beta$), respectively. Then, the angle η of incidence, i.e., the angle between the vectors $-\boldsymbol{\kappa}_0$ and $\boldsymbol{n}$, is determined from the equation

$$\cos\eta = \cos\chi\cos\psi - \sin\varphi\cos\varepsilon\sin\beta. \qquad \text{(A1.1)}$$

Similarly, the angle η' of reflection, i.e. the angle between $\boldsymbol{\kappa}$ and $\boldsymbol{n}$, is

$$\cos\eta = \sin\varphi\sin\chi\sin\varepsilon\sin\beta - \cos\varphi\sin\chi\cos\varepsilon\sin\beta + \cos\chi\cos\beta. \qquad \text{(A1.2)}$$

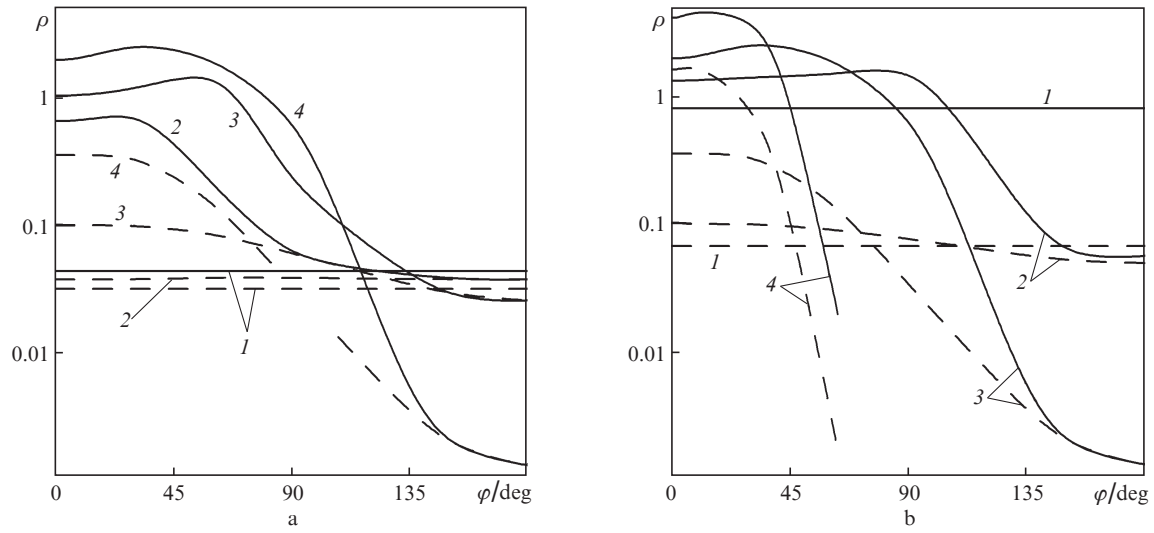

Figure 4. Azimuth structure of the luminance factors of reflected light upon illumination of the medium from outside (dashed curves) and inside (solid curves); $\psi =$ (a) 60° and (b) 80°, $\chi =$ (*1*) 0, (*2*) 30°, (*3*) 60° and (*4*) 80°.

From the law of geometrical optics (angle of incidence equals the angle of reflection), equating the right-hand sides of (A1.1) and (A1.2), we obtain the first equation for the unknown β and ε.

The equation for the plane of incidence passing through $\boldsymbol{\kappa}_0$ and $\boldsymbol{n}$ has the form

$$\begin{vmatrix} x & y & z \\ 0 & \sin\psi & -\cos\psi \\ \sin\varepsilon\sin\beta & \cos\varepsilon\sin\beta & \cos\beta \end{vmatrix} = 0. \qquad \text{(A1.3)}$$

The equation for the plane of reflection passing through $\boldsymbol{\kappa}$ and $\boldsymbol{n}$ has the form

$$\begin{vmatrix} x & y & z \\ \sin\varphi\sin\chi & \cos\varphi\sin\chi & \cos\chi \\ \sin\varepsilon\sin\beta & \cos\varepsilon\sin\beta & \cos\beta \end{vmatrix} = 0. \qquad \text{(A1.4)}$$

From another law of geometrical optics [the incident and reflected beams as well as the normal to the micro surface lie in the plane defined by (A1.3) and (A1.4)] we have the second equation for β and ε. Solving the system of two equations with two unknowns, we obtain relations (20)–(22).

Appendix 2

Relationship between solid angles $\Delta\omega_s$ and $\Delta\omega$

Let the reflected light flux be recorded in a small solid angle. We find the solid angle $\Delta\omega$, within which there are normals to the micro areas reflecting light in the angle $\Delta\omega_s$. To this end, we turn the reference coordinate system xyz (see Fig. 1) so that the z' axis of the new coordinate system, $x'y'z'$, be oriented along the axis of the solid angle $d\omega_s$, and the incident light beam have, as before, the azimuth $\varphi_0' = 0$. Let us denote the corresponding angles in the rotated coordinate system, ψ', χ', φ', β' and ε', and because of the smallness of $\Delta\omega_s$ we will have $\chi' \ll 1$. The magnitude of the solid angle is obviously independent of the coordinate system, and therefore

$$\Delta\omega = \iint\limits_{\Sigma} \sin\beta\, d\beta\, d\varepsilon = \iint\limits_{\Sigma} \sin\beta'\, d\beta'\, d\varepsilon', \qquad \text{(A2.1)}$$

where integration is performed over the angles corresponding to the area Σ of the segment cut by the solid angle $\Delta\omega$ on the sphere, shown in Fig. 1. We will change the variables $\beta' = \beta'(\chi', \varphi')$, $\varepsilon' = \varepsilon'(\chi', \varphi')$ in the second integral of (A2.1). In other words, we pass from integration over β' and ε' to integration over χ' and φ'. Then, (not to load the text with details, we omit the primes in the angles, meaning that all the angles below refer the rotated coordinate system $x'y'z'$)

$$\Delta\omega = \iint\limits_{\Sigma_s} \sin[\beta(\chi,\varphi)]\sqrt{EG - F^2}\, d\chi d\varphi, \qquad \text{(A2.2)}$$

where integration is performed over the angles corresponding to the area Σ_s of the segment cut by the solid angle $\Delta\omega_s$ on the sphere, shown in Fig. 1,

$$E = \left(\frac{\partial\beta}{\partial\chi}\right)^2 + \left(\frac{\partial\varepsilon}{\partial\chi}\right)^2, \quad G = \left(\frac{\partial\beta}{\partial\varphi}\right)^2 + \left(\frac{\partial\varepsilon}{\partial\varphi}\right)^2,$$
$$F = \frac{\partial\beta}{\partial\chi}\frac{\partial\beta}{\partial\varphi} + \frac{\partial\varepsilon}{\partial\chi}\frac{\partial\varepsilon}{\partial\varphi}. \qquad \text{(A2.3)}$$

We now use relations (20)–(22) and take into account that $\chi \ll 1$. Then after neglecting the terms with a higher order smallness that χ, these formulas take the form

$$\tan\beta = \frac{\cos\psi - 1}{\sin\varepsilon\sin\varphi\sin\chi + \cos\varepsilon(\cos\varphi\sin\chi + \sin\psi)}, \qquad \text{(A2.4)}$$

$$\tan\varepsilon = -\frac{\sin\varphi\sin\chi}{\sin\psi}. \qquad \text{(A2.5)}$$

Using (A2.4) and (A2.5) we compute the partial derivatives

$$\frac{\partial\beta}{\partial\chi} = 0.5\cos\varphi, \quad \frac{\partial\varepsilon}{\partial\chi} = -\frac{\sin\varphi}{\sin\psi},$$
$$\frac{\partial\beta}{\partial\varphi} = -0.5\sin\chi\sin\varphi, \quad \frac{\partial\varepsilon}{\partial\varphi} = -\frac{\sin\chi\cos\varphi}{\sin\psi}, \qquad \text{(A2.6)}$$

substitute them in (A2.3) and, as a result, obtain

$$EG - F^2 = \frac{\sin^2\chi}{4\sin^2\psi}. \qquad \text{(A2.7)}$$

In addition, with accuracy up to terms of order χ, we have $\sin\beta = \sin\psi/2$. Substituting this equality and (A2.7) into (A2.2) we finally obtain

$$\Delta\omega = \iint\limits_{\Sigma_s} \sin(\psi/2)\frac{\sin\chi}{2\sin\psi}\mathrm{d}\chi\mathrm{d}\varphi = \frac{\Delta\omega_s}{4\cos(\psi/2)}. \qquad \text{(A2.8)}$$

It follows from (23) that at $\chi \ll 1$ the angle η of incidence, independent of the choice of the coordinate system, is equal to $\psi/2$. Finally, we obtain the desired relation between the solid angles $\Delta\omega$ and $\Delta\omega_s$ in the form of (24).

References

1. Ivanov A.P., Barun V.V. *Inzh.-Fiz. Zh*., **84** (1), 22 (2011) [*J. Eng. Phys. Thermophys*., **84** (1), 23 (2011)].
2. Lu J.O., Hu X.-H., Dong K. *Appl. Opt*., **39** (31), 5890 (2000).
3. Meglinski I.V., Matcher S.J. *Opt. Spektrosk*., **91** (4), 692 (1998) [*Opt. Spectrosc*., **91** (4), 654 (1998)].
4. Meglinski I.V. *Kvantovaya Elektron*., **31** (12) (2001) [*Quantum Electron*., **31** (12) 1101 (2001)].
5. Meglinski I.V., Matcher S.J. *Physiol. Measurem*., **23** (4), 741 (2002).
6. Isakovich M.A. *Zh. Eksp. Teor. Fiz*., **23** (3), 305 (1952).
7. Bass F.G., Fuks I.M. *Wave Scattering From Statistically Rough Surfaces* (Oxford: Pergamon Press, 1979; Moscow: Nauka, 1972).
8. Fedoryuk M.V. *Asimptotika: integraly i ryady* (Asymptotics: Integrals and Series) (Moscow: Nauka, 1987).
9. Rogatkin D.A. *Opt. Spektrosk*., **97** (3), 484 (2004).
10. Leontovich M.A. *Issledovaniya po rasprostraneniyu radiovoln* (Investigations of Propagation of Radio-Waves). Ed. by B.A. Vvedenskii (Moscow: Izd. Akad. Nauk SSSR, 1948) Pt. 2, p. 5.
11. Maradudin A.A., Mendez E.R. *Opt. Spektrosk*., **80** (3), 459 (1996) [*Opt. Spectrosc*., **80** (3), 409 (1996)].
12. Barun V.V., Ivanov A.P. *Inzh.-Fiz. Zh*., **85** (5), 1117 (2012) [*J. Eng. Phys. Thermophys*., **85** (5), 1215 (2012)].
13. Brekhovskikh L.M. *Dokl. Akad. Nauk SSSR*, **79** (4), 585 (1951); *Zh. Eksp. Teor. Fiz*., **23** (3), 275 (1952).
14. Varanovich A.G. *Akust. Zh*., **53** (3), 346 (2007).
15. Chaevskii E.V. *Izv. Vyssh. Uchebn. Zaved., Ser. Radiofiz*., **8** (6), 1128 (1965).
16. Smith B.G. *IEEE Trans. Antennas Propag*., **15** (5), 668 (1967).
17. Ivanov A.P. *Optika rasseivayushchikh sred* (Optics of Scattering Media) (Minsk: Nauka i Tekhnika, 1969).
18. Korn G., Korn T. *Mathematical Handbook for Scientists and Engineers* (New York: McGraw-Hill, 1961; Moscow: Nauka, 1977).
19. Mullamaa Yu.-A.R. *Atlas opticheskikh kharakteristik vzvolnovannoi poverkhnosti morya* (Atlas of the Optical Characteristics of the Rough Sea Surface) (Tartu: Izd. Akad Nauk ESSR, 1964).
20. Toporets A.S. *Optika sherokhovatoi poverkhnosti* (Optics of a Rough Surface) (Leningrad: Mashinostroenie, 1988).
21. Tuchin V.V. *Lazery i volokonnaya optika v biomeditsinskikh issledovaniyakh* (Lasers and Fibre Optics in Biomedical Research) (Saratov: Izd. Saratov. Univer., 1998).